Iron Tris(bipyridine)-Centered Poly(ethylene glycol)-Poly(lactic acid) Star Block Copolymers

Gina L. Fiore, Jessica L. Klinkenberg, and Cassandra L. Fraser*

Department of Chemistry, University of Virginia, McCormick Road, P.O. Box 400319, Charlottesville, Virginia 22904-4319

Received July 29, 2008; Revised Manuscript Received August 27, 2008

ABSTRACT: Block copolymers incorporating biocompatible poly(ethylene glycol) (PEG) and poly(lactide) (PLA) polymers and labile metal complexes can serve as stimuli responsive biomaterials. Bipyridine-centered PEG-PLA materials were prepared via ring opening polymerization of ethylene oxide and lactide (D,L and L). Macroligands and their iron complexes $[Fe\{bpy(PEG\text{-}PLA)_2\}_3]Cl_2$ were characterized by gel permeation chromatography, ^1H NMR, and UV−vis spectroscopy. Solvent and counterion effects were also explored by UV−vis spectroscopy. Extinction coefficients drop 3-fold in CH_2Cl_2; values typical for iron(II) tris(bipyridine) complexes are restored by addition of very small quantities of MeOH. Thermal properties of $bpy(PEG\text{-}PLA)_2$ and $[Fe\{bpy(PEG\text{-}PLA)_2\}_3]^{2+}$ were investigated by thermogravimetric analysis and differential scanning calorimetry, showing values typical for the polymer blocks and little effect of incorporated ligand or metal sites. Micelle-like nanoparticles of block copolymer macroligands and iron star polymer complexes were prepared via nanoprecipitation. Dynamic light scattering and transmission electron microscopy analyses confirm the presence of spheroid particles (macroligands, 111−253 nm in diameter; iron complexes, 37−75 nm in diameter).

Introduction

Block copolymers with hydrophilic poly(ethylene glycol) (PEG) and hydrophobic poly(lactic acid) (PLA) segments are common in biomedical applications. These amphiphilic materials have been fabricated as micelles,[1−7] nanoparticles,[5,8−11] hydrogels,[12−18] and fibers[19,20] for drug delivery and tissue engineering. PLA degrades over time via cleavage of the polyester chain; however, degradation can take several months.[21] The combination of hydrophobic PLA with hydrophilic PEG can result in a significant increase in degradation rates.[3,18] The introduction of metals into biomaterials can also alter degradation as well as bioactivity. For example, iron plays many roles in biological systems, both beneficial as an essential element and detrimental in promoting reactive oxygen species (ROS) formation;[22,23] however, selective targeting of damaging reactive species to pathological tissues is a common strategy in medicine.[24−26] Additionally, from a biomaterials design standpoint, metal centers can serve as stimuli responsive cross-links. Iron release and generation of reactive species can facilitate polymer degradation, thus serving as an additional method of modulating materials fragmentation and drug release. As reported for the polymeric metal complex (PMC) $[Fe(bpyPEG_2)_3]SO_4$, dissociation of the $bpyPEG_2$ macroligands results in a 3-fold decrease in molecular weight, and the released metal, in turn, facilitates polymer backbone degradation in aqueous solution, presumably via a radical mechanism.[27,28] Here we extend the initial study with PEG to metal site-isolated, iron tris(bipyridine)-centered PEG-PLA materials to gain a better understanding of the effects of metal complexes on biomaterials properties and the ways that these common biomaterials influence metal complex reactivity. The synthesis, UV−vis spectroscopic studies, thermal analysis, and nanoparticle fabrication of $[Fe\{bpy(PEG\text{-}PLA)_2\}_3]Cl_2$ materials are described (Figure 1).

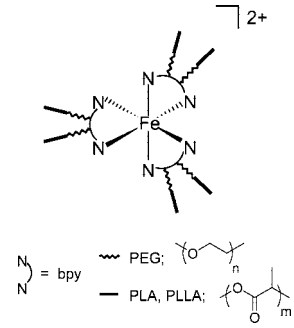

Figure 1. Schematic representation of iron(II) tris(bipyridine)-centered star block copolymer with PEG-PLA block copolymer arms.

Experimental Section

Materials. The difunctional initiator 4,4′-bis(hydroxymethyl)-2,2′-bipyridine ($bpy(CH_2OH)_2$) was prepared as previously reported.[29] 3,6-Dimethyl-1,4-dioxane-2,5-dione (D,L-lactide; Aldrich) and (3*S*)-*cis*-3,6-dimethyl-1,4-dioxane-2,5-dione (L-lactide) were recrystallized from ethyl acetate (2×) and stored in a drybox under a nitrogen atmosphere. Ethylene oxide (EO) (*caution*, Aldrich) was dried over dibutyl magnesium (Aldrich), distilled under reduced pressure (2×), and stored in an air-free buret. Potassium naphthalenide was prepared by reaction of potassium and naphthalene in THF and titrated (3×) with a standardized HCl solution.[30] Iron(II) tetrafluoroborate (Aldrich) and iron(II) chloride (Strem) were titrated with 2,2′-bipyridine (Aldrich) prior to use to verify the concentration of ferrous ions. Tetrahydrofuran and methylene chloride (Fisher) were purified by passage through alumina columns.[31] Methanol (Fisher) was purged with argon for iron reactions. Chloroform-*d* ($CDCl_3$) was passed through a short plug of dry, activated (Brockman I) basic alumina prior to use. Tin(II) 2-ethylhexanoate ($Sn(oct)_2$; Spectrum) and all other reagents were used as received.

Methods. ^1H NMR (300 MHz) spectra were recorded on a Varian UnityInova spectrometer in $CDCl_3$ unless indicated otherwise. ^1H NMR coupling constants are given in hertz. Resonances were referenced to the signal for residual protiochloroform at 7.260 ppm. UV−vis spectra were recorded on a Hewlett-Packard 8452A diode-array spectrophotometer in CH_2Cl_2/CH_3OH (3:1) unless indicated otherwise. Molecular weights were determined by gel permeation chromatography (GPC) (THF, 25 °C, 1.0 mL/min) using multiangle laser light scattering (MALLS) (λ = 633 nm, 25 °C) and refractive index (RI) (λ = 633 nm, 40 °C) detection. A Polymer Laboratories 5 μm mixed-C guard column and two GPC columns

* To whom correspondence should be addressed. E-mail: fraser@virginia.edu.

10.1021/ma801721q CCC: $40.75
Published on Web 11/12/2008

along with Wyatt Technology Corp. (Optilab DSP interferometric refractometer, DAWN DSP laser photometer) and Agilent Technologies (series 1100 HPLC) instrumentation and Wyatt Technology software (ASTRA) were used in GPC analysis. Incremental refractive indices (d*n*/dc values) for copolymers were estimated by a single-injection method that assumed 100% mass recovery from the columns. Thermogravimetric analysis (TGA) was conducted using a TA Instruments TGA 2050 thermogravimetric analyzer from 30 to 500 °C with a heating/cooling rate of 10 °C/min under N_2. Differential scanning calorimetry (DSC) measurements were performed using a TA Instruments DSC 2920 modulated differential scanning calorimeter. Analyses were carried out in modulated mode under a nitrogen atmosphere (amplitude ±1 °C, period 60 s, heating rate 5 °C/min, range −10 to +200 °C or −10 to +150 °C). Reported values of thermal events are from the second heating cycle and the reverse heat flow curve unless indicated otherwise (T_d = onset point of decomposition, T_m reported as the peak maximum). Nanoparticle suspensions were analyzed using dynamic light scattering (DLS) (90° angle) on a Photocor Complex (Photocor Instruments Inc.) equipped with a He−Ne laser (Coherent, California, model 31-2082, 633 nm, 10 mW). Sizes and polydispersities were determined using DynaLS software (Alango, Israel). Nanoparticle morphologies were analyzed by transmission electron microscopy (TEM); drops of the diluted nanoparticle suspension (20 μL in 10 mL of deionized water) were deposited directly onto carbon-coated electron microscope grids and then allowed to dry. TEM was performed using a JEOL 200CX, tungsten filament, operated at 200 kV using low-dose conditions required by the beam sensitivity of the material. Bright-field images were taken using a CCD camera (AMT).

BpyPLA$_2$. The macroligand was prepared as previously described with the following modification. A catalyst loading of 1:50 per initiation site was used instead of 1:75 as previously reported.[32] The following reagent loadings were used: bpy$(CH_2OH)_2$ (0.021 g, 0.097 mmol), D,L-lactide (0.904 g, 6.27 mmol), and Sn$(oct)_2$ in hexanes (94 μL, 131 mM, 3.8 μmol). BpyPLA$_2$ was obtained as a white solid, 0.739 g (80% uncorrected for monomer conversion). Spectral properties were in accord with those previously reported.[32] M_w(MALLS) = 10 000, PDI = 1.05, and d*n*/dc = 0.050 mL/g.

BpyPEG$_2$, 1. A representative preparation is provided. The polymerization was performed in a 250 mL glass reactor equipped with three internal Ace-Threds threaded glass connectors and a glass-covered stir bar. (See Supporting Information Figure S1 for an image of the reaction apparatus.) Using Teflon ferrules, nylon bushings, and FETFE O-rings, the reactor was fitted with a glass plug, a Teflon valve, and a glass Y-connector. The Y-connector was equipped with a Teflon valve, a purge valve, a compound gauge, and a port capped with a Teflon-coated septum. The valve on the Y-connector was connected to a vacuum/nitrogen manifold. The apparatus was evacuated to $\sim 10^{-3}$ Torr, flame-dried, and backfilled with N_2 (3×). An air-free pretared buret containing EO was then attached to the Teflon valve on the reaction flask with flexible metal tubing equipped with Swagelok unions and Teflon ferrules. The buret was kept cold in an ice H_2O bath. The apparatus and metal tubing were evacuated and backfilled with N_2 (4×). A solution of bpy$(CH_2OH)_2$ (0.200 g, 0.925 mmol) in THF (20 mL) was added to the reaction flask through the Teflon-coated septum using a N_2-flushed syringe. Additional THF was added to establish an initiator concentration of 18−20 mM. Potassium naphthalenide (4.0 mL of a 0.23 M solution, 0.925 mmol) was then added dropwise. The reaction apparatus was isolated from the manifold under a N_2 atmosphere and then cooled to −78 °C. The EO (9.24 g, 210 mmol) was added to the reaction mixture. The Teflon valves to the buret and reaction flask were then sealed, and the metal tubing and EO buret were removed. The reaction mixture was removed from the ice bath, warmed to room temperature, and then slowly warmed to 40 °C by immersion in an oil bath, upon which the pressure increased significantly. The reaction pressure (i.e., EO monomer consumption) was monitored via the attached compound gauge (below ~10 psi deemed safe; above ~10 psi the pressure is released via the purge valve). When the pressure dropped to ~3 psi, the reaction flask was cooled to room temperature. An acidic methanol solution (1 mL of a stock solution containing 1.5 mL concentrated HCl in 25 mL of methanol) was added to the dark green solution through the glass plug port. The resulting golden yellow-brown mixture was stirred at room temperature for 2 h, then passed through a neutral alumina plug, concentrated in vacuo, and precipitated from a minimal amount of CH_2Cl_2 into cold diethyl ether (~250 mL, −78 °C). The resulting white solid was collected by filtration, washed with cold diethyl ether, and dried in vacuo, 7.26 g (79% uncorrected for monomer conversion). ^{1}H NMR (300 MHz, $CDCl_3$): δ 8.64 (d, J = 4.9 Hz, H-6, H-6′), 8.32 (s, H-3, H-3′), 7.37 (dd, J = 5.0 Hz, J = 1.3 Hz, H-5, H-5′), 4.67 (s, bpy CH_2), 3.64 (m, PEG CH_2CH_2), 2.57 (t, J = 6.2 Hz, CH_2CH_2OH). M_w(MALLS) = 12 100, PDI = 1.04, and d*n*/dc = 0.066 mL/g.

Bpy(PEG-PLA)$_2$, 2. A representative procedure is provided. BpyPEG$_2$ (0.650 g, 0.138 mmol, M_n = 4700) and D,L-lactide (0.650 g, 4.51 mmol) were combined in a Kontes flask. The flask was evacuated, backfilled with nitrogen, sealed, and placed in an oil bath at 130 °C to create a homogeneous melt. Under a flow of nitrogen, a 56.0 mM solution of Sn$(oct)_2$ in hexanes (99 μL, 5.5 μmol) was added to the reaction mixture. The reaction vessel was resealed and heated at 130 °C until an extremely viscous mixture resulted (~1.5 h). The reaction mixture was cooled to room temperature, dissolved in a minimal amount of CH_2Cl_2, and precipitated by dropwise addition to cold stirring hexanes (−78 °C). The supernatant was decanted, and the solid residue was precipitated (2×) from CH_2Cl_2/MeOH (−78 °C), washed with cold methanol, and dried in vacuo to afford bpy(PEG-PLA)$_2$ as an off-white solid, 1.09 g (84% uncorrected for monomer conversion). ^{1}H NMR (300 MHz, $CDCl_3$): δ 8.67 (m, H-6, H-6′), 8.36 (m, H-3, H-3′), 7.41 (m, H-5, H-5′), 5.10−5.28 (m, CH), 4.70 (s, bpy CH_2), 4.40−4.20 (m, CH(CH$_3$)OH, RCH_2CO$_2$), 3.64 (m, PEG CH_2CH_2), 2.71 (br s, O H), 1.64−1.42 (m, CH_3). M_w(MALLS) = 13 700, PDI = 1.11, and d*n*/dc = 0.057 mL/g.

Bpy(PEG-PLLA)$_2$, 3. A representative preparation is provided. Macroligands were prepared using the same procedure as described for bpy(PEG-PLA)$_2$ with the following reagent loadings: bpyPEG$_2$ (0.301 g, 0.063 mmol, M_n = 4800), L-lactide (1.20 g, 8.35 mmol), and 32.2 mM Sn$(oct)_2$ in hexanes (164 μL, 5.4 μmol). Bpy(PEG-PLLA)$_2$ was obtained as a white solid, 1.15 g (76% uncorrected for monomer conversion). ^{1}H NMR (300 MHz, $CDCl_3$): δ 8.64 (d, J = 5.0 Hz, H-6, H-6′), 8.32 (s, H-3, H-3′), 7.36 (m, H-5, H-5′), 5.16 (q, J = 7.1 Hz, CH), 4.68 (s, bpy CH_2), 4.38−4.25 (m, RCH(CH$_3$)OH, RCH_2CO$_2$), 3.64 (m, PEG CH_2CH_2), 1.58 (d, J = 7.1 Hz, CH_3), 2.65 (d, J = 6.3 Hz, OH) 1.49 (d, J = 7.0 Hz, RCH(CH_3)OH). M_w(MALLS) = 25 000, PDI = 1.13, and d*n*/dc = 0.052 mL/g.

Kinetics of Polymeric Iron(II) Complex Formation. *Reactions with $FeCl_2$ and $Fe(BF_4)_2$ in CH_2Cl_2/MeOH.* A representative procedure is provided. Under an argon atmosphere, a 1 cm path length cuvette was charged with bpy(PEG-PLA)$_2$ (0.005 g, 0.05 μmol, M_n = 9900), MeOH (0.525 mL), and CH_2Cl_2 (1.875 mL). A portion of the pretitrated iron stock solution (100 μL, 0.017 μmol) was added (resultant solution 3:1 CH_2Cl_2/MeOH), and the reaction was stirred and monitored by UV−vis (2 h).

Reactions with $FeSO_4$ in Water. The formation of the iron(II) PEG-PLA complex was monitored by UV−vis spectroscopy under ambient conditions as previously described with the following reagent loadings:[27] bpy(PEG-PLA)$_2$ (0.006 g, 0.6 μmol, M_n = 9900), $FeSO_4$ (68 μL, 2.99 mM, 0.2 μmol), H_2O (2.54 mL). UV−vis (H_2O): λ_{max}(MLCT) (ε) = 532 nm (9100 M^{-1} cm^{-1}).

Preparative Scale Synthesis of Polymeric Iron Complexes 4 and 5. A representative procedure is provided. A portion of the pretitrated methanol stock solution of $FeCl_2 \cdot 4H_2O$ (4.9 mL, 5.30 mM, 0.026 mmol) was diluted in CH_2Cl_2 (9.7 mL), and a solution of bpy(PEG-PLA)$_2$ (0.700 g, 0.070 mmol, M_n = 9900) in CH_2Cl_2 (5 mL) was added dropwise. The resulting red-violet mixture (3:1 CH_2Cl_2/MeOH) was stirred at room temperature under N_2 for ~15−20 min and then concentrated in vacuo. The crude product was precipitated from CH_2Cl_2/cold MeOH (−78 °C), washed with cold MeOH, and dried in vacuo to provide the iron-centered polymeric complex as a pink solid, 0.635 g (91%). ^{1}H NMR (300

Scheme 1

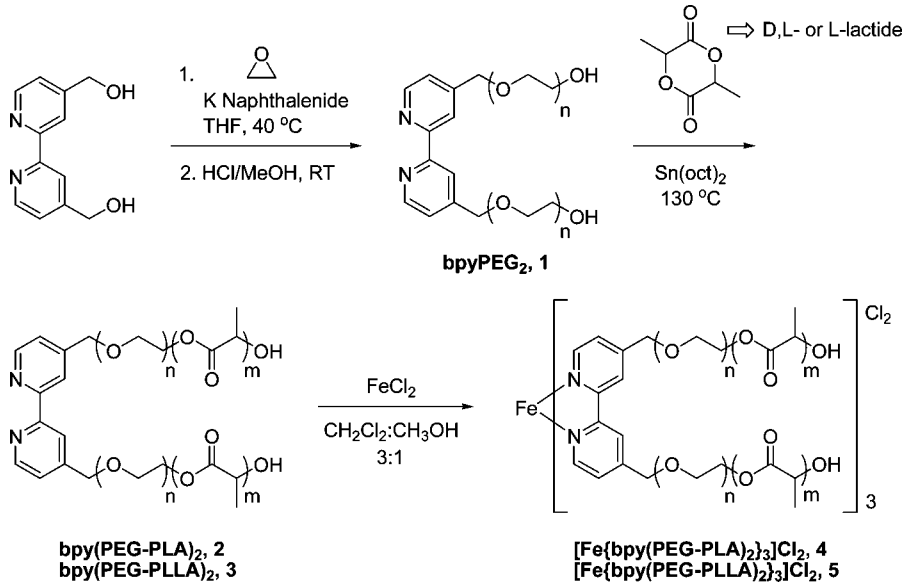

MHz, $CDCl_3$): δ 5.10−5.28 (m, C*H*), 4.40−4.20 (m, C*H*(CH_3)OH), 3.64 (m, PEG CH_2CH_2), 2.71 (br s, O*H*), 1.64−1.42 (m, CH_3). M_n(calcd) = 29 800. UV−vis (3:1 CH_2Cl_2/MeOH): λ_{max}(MLCT) (ε) = 531 nm (12 300 M^{-1} cm^{-1}).

Nanoparticle Fabrication. A representative procedure is provided. A solution of [Fe{bpy(PEG-PLA)$_2$}$_3$]Cl_2 (0.051 g, 0.001 mmol, M_n = 36 900) was prepared in DMSO (5 mL) and added dropwise to distilled water (50 mL) with stirring. After 30 min, the suspension was introduced into a dialysis tube (MWCO 12000−14000) and dialyzed against distilled water overnight. The resulting pink solution was then freeze-dried for characterization by NMR, GPC, and UV−vis spectroscopy. Nanoparticle sizes were determined by DLS, and the morphologies were visualized by TEM.

Results and Discussion

Bipyridine Macroligands. Bipyridine-centered macroligands, bpyPLA$_2$ and bpyPEG$_2$ homopolymers and bpy(PEG-PLA)$_2$ and bpy(PEG-PLLA)$_2$ block copolymers (PLA = D,L-polymer, PLLA = L-polymer), were prepared via controlled ring opening polymerization methods. BpyPLA$_2$ was synthesized in bulk lactide monomer using bpy(CH_2OH)$_2$ as the initiator and Sn(oct)$_2$ as the catalyst. Previously reported methods employed a catalyst loading of 1:75 per primary alcohol initiation site; however, increasing the loading to 1:50 significantly increased the reaction rates. Targeted molecular weights can be obtained in 10 min versus ~18 h.[32] A nearly linear pseudo-first-order kinetics plot indicates good control to 12 min, after which time the reaction became extremely viscous and slowed down (Figure 2). A plot of molecular weight versus monomer conversion shows that the molecular weight distributions remain narrow even to high conversion (Figure 3).

Previously, we reported the synthesis of bpyPEG$_2$ macroligands via anionic ring opening polymerization of ethylene oxide from a bpy(CH_2OH)$_2$ initiator.[27] Although materials were obtained in good yield (~75%) with low molecular weight distributions (PDI ≤ 1.1), a low molecular weight shoulder was present in GPC traces of all samples. Thus, reaction conditions were optimized to obtain materials with improved molecular weight control. Initiator concentration and equivalents of base per initiation site are important factors.[27] In this study, a custom-built air-free reaction system was used both for more rigorous monomer purification by sequential vacuum distillations from dibutylmagnesium and for the polymerization (Supporting Information, Figure S1). Modeled after work by Hillmyer,[33] PEG was grown from the bpy(CH_2OH)$_2$ initiator in the presence of potassium naphthalenide in THF at 40 °C (Scheme 1). The reaction pressure was monitored using a compound gauge for safety reasons and to provide a relative measure of EO consumption. Complete monomer conversion with good control is possible for PEG polymerizations.[34] Once a minimum pressure (~3 psi) was reached, the reaction was cooled to room temperature, vented, and then quenched with acidic methanol solution. The mixture was stirred for an additional 2 h and

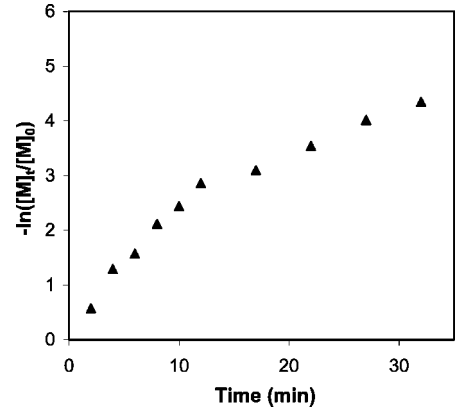

Figure 2. Kinetics plot for the polymerization of D,L-lactide with bpy(CH_2OH)$_2$ initiator (Sn(oct)$_2$:primary alcohol = 1:50).

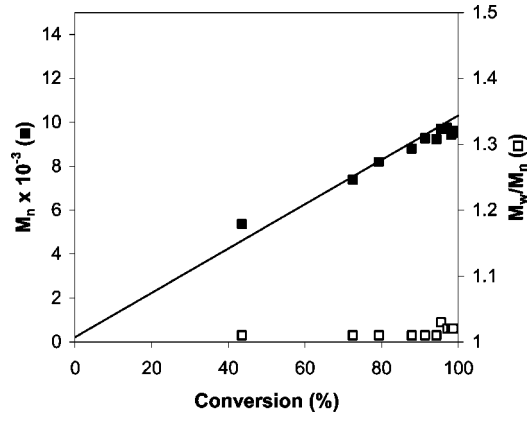

Figure 3. Number-average molecular weight versus percent conversion and polydispersity indices for the polymerization of D,L-lactide with bpy(CH_2OH)$_2$ initiator (Sn(oct)$_2$:primary alcohol = 1:50).

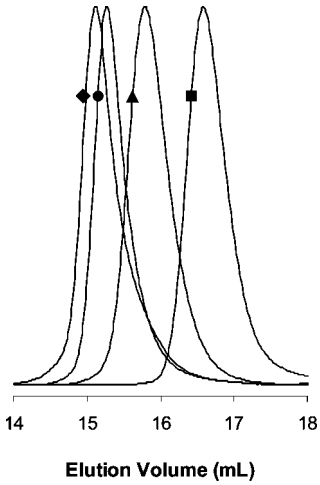

Figure 4. GPC overlay of bpyPEG$_2$ macroligands of increasing molecular weight: (■) M_n = 3200, PDI = 1.03; (▲) M_n = 5700, PDI = 1.03; (●) M_n = 7100, PDI = 1.00; (◆) M_n = 11 600, PDI = 1.04.

Table 1. Molecular Weight Data for bpyPEG$_2$ Macroligands[a]

M_n	M_w	PDI
3200	3300	1.03
4800	4900	1.02
5700	5900	1.03
6200	6500	1.04
7100	7100	1.00
7600	7900	1.04
10000	11600	1.04
11600	12100	1.04

[a] Molecular weights determined by GPC (MALLS, THF) with d*n*/dc = 0.066 mL/g.

passed through a neutral alumina plug, and the solution was precipitated into cold diethyl ether (−78 °C) to afford white bpyPEG$_2$ products in 70−80% yield. As illustrated in Figure 4, the GPC traces corresponding to macroligands of various molecular weights are symmetric (i.e., no shoulders) and molecular weight distributions are very narrow (PDI ≤ 1.05) (Table 1). The resulting polymer products contain a bidentate ligand for metal coordination and OH end groups that can serve as macroinitiators for block copolymer synthesis,[18,35,36] reactive groups for bioconjugation,[37−40] or precursors to acrylate cross-linking reagents for hydrogel synthesis.[28,41−44]

When bpyPEG$_2$ is used as a macroinitiator in combination with D,L- and L-lactide, amphiphilic PEG-PLA (amorphous D,L-polymer) and PEG-PLLA (semicrystalline L-polymer) block copolymers result (Scheme 1). As for PLA homopolymers, kinetics experiments of bpy(PEG-PLA)$_2$ show that the tin-catalyzed bulk polymerization is pseudo-first-order until the reaction mixture becomes extremely viscous and the rate of the reaction decreases (Figure 5). The M_n vs monomer conversion (%) plot is linear, molecular weights are in accord with theoretical values, and PDIs are low (<1.1), all indicative of good reaction control (Figure 6).

A series of bpy(PEG-PLA)$_2$ and bpy(PEG-PLLA)$_2$ macroligands with varying degrees of polymerization for PEG and PLA segments and overall molecular weights ranging from 9000 to 38 500 were synthesized (Table 2). Provided that targeted PLA blocks had molecular weights <20 000, GPC traces of the block copolymers were symmetric and PDIs were typically <1.2, suggesting efficient initiation from the PEG macroinitiator (Figure 7). However, when higher molecular weight PLA blocks were targeted (>20 000), low molecular shoulders were evident in GPC traces. Control reactions of PLA-PEG-PLA with commercially available HO-PEG-OH as the macroinitiator also

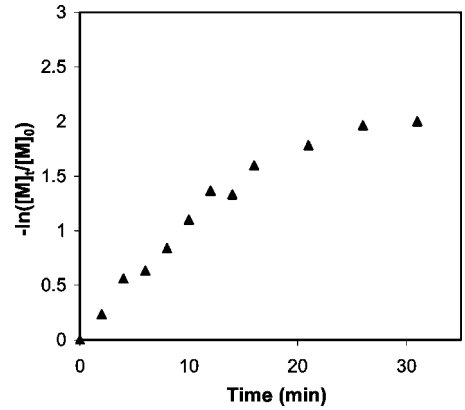

Figure 5. Kinetics plot for the bulk polymerization of D,L-lactide with bpyPEG$_2$ macroinitiator (Sn(oct)$_2$:primary alcohol = 1:50). Molecular weights were estimated with d*n*/dc = 0.050 mL/g of PLA.

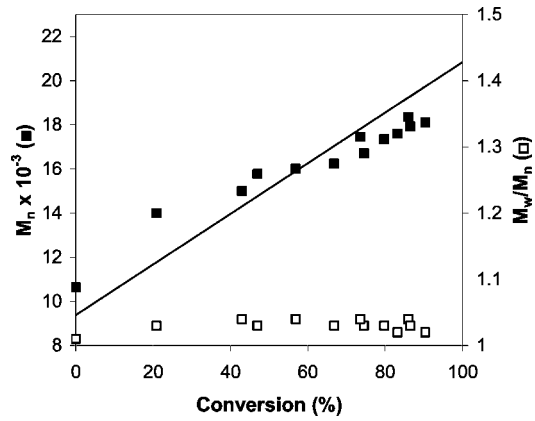

Figure 6. Number-average molecular weight versus percent conversion and polydispersity indices for the polymerization of D,L-lactide with bpyPEG$_2$ macroinitiator (Sn(oct)$_2$:primary alcohol = 1:50). Molecular weights were estimated with d*n*/dc = 0.050 mL/g of PLA.

Table 2. Molecular Weight Data for bpy(PEG-PLA)$_2$ and bpy(PEG-PLLA)$_2$ Block Copolymers

	first block[a]			triblock		
polymer	M_n	M_w	PDI	M_n	M_w	PDI
bpy(PEG-PLA)$_2$	5700	5900	1.03	10000[b]	11100[b]	1.11
				12300[c]	13700[c]	1.11
				38500[d]	44400[d]	1.15
	6200	6500	1.04	12500[b]	14700[b]	1.17
				19100[e]	22600[e]	1.18
				39600[f]	47700[f]	1.20
	11700	12100	1.04	22600[g]	26800[g]	1.18
bpy(PEG-PLLA)$_2$	4800	4900	1.02	9100[h]		1.11
				14600[i]	18700[i]	1.28
				22900[j]	25000[j]	1.13

[a] Molecular weights determined using GPC (MALLS, THF) with d*n*/dc = 0.066 mL/g. [b] d*n*/dc = 0.058 mL/g. [c] d*n*/dc = 0.057 mL/g. [d] d*n*/dc = 0.048 mL/g. [e] d*n*/dc = 0.052 mL/g. [f] Molecular weight estimated using PLA d*n*/dc = 0.050 mL/g. [g] d*n*/dc = 0.054 mL/g. [h] Molecular weight determined by ^{1}H NMR via relative integrations of PEG -C*H*$_2$C*H*$_2$- (3.64 ppm) vs PLLA -C*H*- (5.16 ppm). GPC values were inaccurate for low molecular weight PEG-PLLA block copolymers. [i] Molecular weight estimated using PEG d*n*/dc = 0.066 mL/g. [j] d*n*/dc = 0.052 mL/g.

exhibited low molecular weight shoulders under these conditions. This was true regardless of monomer conversion, even when polymerizations were stopped prior to completion.

Polymer products were investigated by ^{1}H NMR analysis. Modification of bpyPEG$_2$ chain ends with PLA is evidenced by the disappearance of the PEG terminal OH at 2.67 ppm and the appearance of a multiplet at 4.20−4.40 ppm corresponding to PLA −RC*H*$_2$CO$_2$− and RC*H*(CH$_3$)OH chemical shifts.

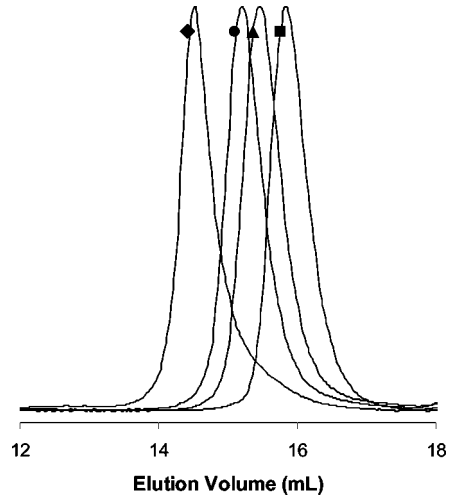

Figure 7. GPC overlay of bpyPEG$_2$ and bpy(PEG-PLA)$_2$ macroligands of increasing PLA molecular weight: bpy(PEG)$_2$ (■) M_n = 5700, PDI = 1.03; bpy(PEG-PLA)$_2$ (▲) M_n = 10 000, PDI = 1.11; (●) M_n = 12 300, PDI = 1.11; (♦) M_n = 38 500, PDI = 1.15.

Table 3. UV−Vis Data for Polymeric Iron(II) Tris(bipyridine) Complexes Formed in Situ

polymeric iron complex[a]	M_n, macroligand	M_n(calcd), Fe PMC[b]	ε^c (M^{-1} cm^{-1})
[Fe{bpy(PEG-PLA)$_2$}$_3$](BF$_4$)$_2$	19100	57500	9270
[Fe{bpy(PEG-PLA)$_2$}$_3$]Cl$_2$	10000	30100	10380
	12300	37000	10630
	19100	57400	10770
	38500	115600	11100

[a] Complexes were prepared in 3:1 CH_2Cl_2/CH_3OH and monitored by UV−vis spectroscopy for 2 h. Maximum values were reached after ∼5 min. [b] Calculated molecular weight of the complex including associated BF_4^- and Cl^- counterions. [c] Extinction coefficients calculated from the maximum absorbance of the MLCT band (λ_{max} = 530 nm) obtained after stirring 3:1 macroligand/FeX_2.

PLLA, from L-lactide, is a stereoregular polymer, whereas PLA, from D,L-lactide, is a stereorandom polymer, resulting in differences in chemical shifts for the −C*H*− groups (PLA, multiplet, 5.10−5.28 ppm; PLLA, quartet, 5.16 ppm). Bpy initiator peaks are only evident in lower molecular weight samples (<19 100). Relative integrations of the PEG −CH_2CH_2− peaks (3.64 ppm) versus PLA and PLLA −C*H*− signals were used to calculate the molecular weights of the block copolymers and are in good agreement with GPC analysis.

Block Copolymer Complexes. To determine the optimal conditions for block copolymer synthesis, kinetics experiments were performed using UV−vis spectroscopy to monitor complex formation. Chelation experiments were performed as previously described,[45] but under argon rather than ambient conditions. Specifically, a pretitrated methanol solution of $FeCl_2 \cdot 4H_2O$ was added via syringe to a 1 cm air-free cuvette containing a macroligand solution in CH_2Cl_2, resulting in a 3:1 CH_2Cl_2/MeOH reaction mixture. The change in absorbance of the MLCT band (λ_{max} = 530 nm) was monitored every 5 min for 2 h. Iron(II) tris(bipyridine)-centered polymeric complexes [Fe{bpy(PEG-PLA)$_2$}$_3$]$^{2+}$ and [Fe{bpy(PEG-PLLA)$_2$}$_3$]$^{2+}$, form within minutes (∼5−10 min), and the molar absorptivities are comparable to that of the [Fe(bpy)$_3$]Cl$_2$ parent compound (ε_{MLCT} = 9420 M^{-1} cm^{-1}) (Table 3). Furthermore, the complexes are stable for 2 h. This contrasts with certain other iron tris(bipyridine) homopolymer and block copolymer complexes that took longer to form[45,46] and degraded[27] under ambient conditions. Modeling preparative scale reactions after kinetics experiments, a solution of bpy(PEG-PLA)$_2$ in CH_2Cl_2 was added dropwise to a solution of iron(II) chloride in CH_2Cl_2/MeOH (Scheme 1).[45,46] The reaction mixture immediately turned a red-violet color and was stirred for ∼20 min at room temperature to ensure complete coordination. Polymeric iron complexes were purified by precipitation from CH_2Cl_2 into cold MeOH (−78 °C). In cases where the PLA segment is small (<19 000 Da triblock), iron complexes were purified by precipitation into cold diethyl ether (−78 °C).

Table 4. UV−Vis Data for Polymeric Iron(II) Complexes Formed in Preparative-Scale Reactions

		CH_2Cl_2/MeOH (3:1)		CH_2Cl_2	
polymeric iron complex	M_n(calcd), Fe PMC[a]	λ_{max}[b] (nm)	ε^c (M^{-1} cm^{-1})	λ_{max}[b] (nm)	ε^c (M^{-1} cm^{-1})
[Fe(bpyPLA$_2$)$_3$](BF$_4$)$_2$	31700	531	9950	532	9970
[Fe(bpyPLA$_2$)$_3$]Cl$_2$	31600	531	6900	554	1000
[Fe{bpy(PEG-PLA)$_2$}$_3$]Cl$_2$	30100	531	12300	539	2200
	37000	531	11600	539	1900
	115600	531	9890	534	2330
[Fe{bpy(PEG-PLLA)$_2$}$_3$]Cl$_2$	27400	531	9280	536	2000
	43900	531	11100	535	2700
	68800	530	6930	534	2340

[a] Calculated molecular weight of the complex including associated BF_4^- and Cl^- counterions. [b] Wavelength maximum of the MLCT absorbance band. [c] Extinction coefficients were calculated from the maximum absorbance of the MLCT band.

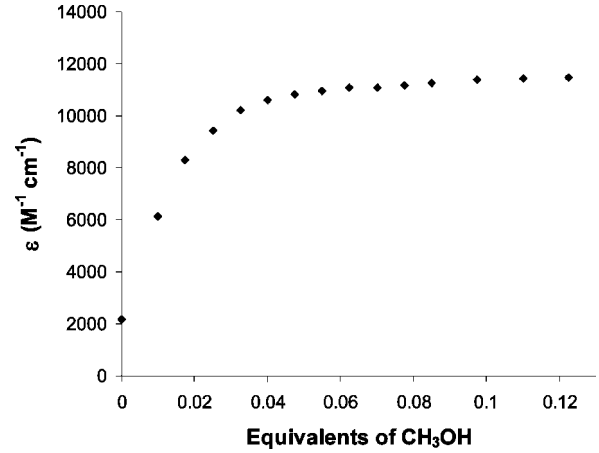

Figure 8. Calculated extinction coefficients (λ_{MLCT}) as a function of methanol addition (20 μL aliquots) to [Fe{bpy(PEG-PLA)$_2$}$_3$]Cl$_2$ in CH_2Cl_2 under argon.

Purified products were evaluated using ^{1}H NMR and UV−vis spectroscopy. ^{1}H NMR spectra of the iron complexes were in accord with those of the respective macroligand precursors. Signals arising from bpyCH_2− aromatic and methylene protons are not evident in the ^{1}H NMR spectra for iron block copolymers. UV−vis analysis was performed in a 3:1 CH_2Cl_2/MeOH cosolvent system. Molar absorptivities of [Fe{bpy(PEG-PLA)$_2$}$_3$]Cl$_2$ and [Fe{bpy(PEG-PLLA)$_2$}$_3$]Cl$_2$ are comparable to that of the Fe tris(bpy) parent compound, further verifying the high quality of the macroligand synthesis and resulting polymeric iron complex materials (Table 4).

Interestingly, when the polymeric iron complexes were dissolved in CH_2Cl_2, a very pale purple solution resulted. Upon addition of MeOH, the red-violet color indicative of the tris complex MLCT transition reappeared (see the Supporting Information). This observation was further explored using UV−vis spectroscopy to monitor spectral changes upon addition of increasing aliquots of MeOH to a CH_2Cl_2 solution of [Fe{bpy(PEG-PLA)$_2$}$_3$]Cl$_2$ (M_n = 30 100) (Figure 8). An overlay of the absorbance spectra before and after MeOH addition is presented in Figure 9. In CH_2Cl_2 solution, the MLCT band at 540 nm is broad and the molar absorptivity is low (2190 M^{-1} cm^{-1}). Upon addition of a very small amount of MeOH (20 μL, 0.01 equiv vs CH_2Cl_2, 2950 equiv vs Fe^{2+}), the MLCT

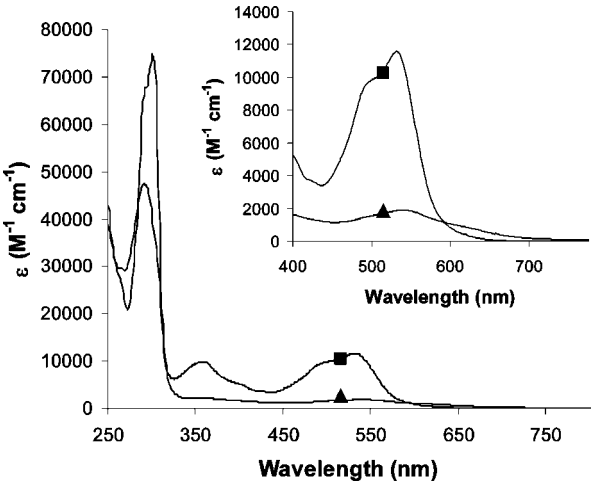

Figure 9. UV−vis spectral overlay of [Fe{bpy(PEG-PLA)$_2$}]Cl$_2$ in CH_2Cl_2 (▲) and 3:1 CH_2Cl_2/MeOH (■). Inset: MLCT absorption band.

absorption band shifted to 533 nm and the molar absorptivity increased 3-fold (6140 M^{-1} cm^{-1}). Additional aliquots resulted in a further increase in absorbance, which reached a plateau at $\varepsilon \approx 11\ 500\ M^{-1}cm^{-1}$ (Figure 8).

To better understand this peculiar solvent effect, counterion and polymer effects were further explored. It is known that counterions can affect polymeric metal complex solubility and complex formation. For example, ruthenium bis(terpyridine)-centered PEG-polystyrene block copolymer[47] with a chloride counterion is soluble in methanol but insoluble in acetone. With a PF_6^- counterion the solubility is reversed; materials are insoluble in methanol and soluble in acetone. For iron complexes, attempts to generate $[Fe(bpyPLA_2)_3]^{2+}$ from $Fe(NH_4)_2(SO_4)_2 \cdot 6H_2O$ and $bpyPLA_2$ produced a pale pink solution, not the expected deep red-violet solution. Only after addition of NH_4PF_6 did the iron tris($bpyPLA_2$) complex form efficiently.[32] This observation prompted us to undertake a systematic study of iron PMCs with different counterions to see whether the reactant/product equilibrium varied for other polymers and metal salts as well.[46] Bpy-centered macroligands based on PtBA, PLA, PCL, and PS were combined with iron(II) salts with I^-, Br^-, PF_6^-, BF_4^-, and ClO_4^- counterions.[46] However, regardless of the counterion, similar high molar absorptivities were obtained, suggestive of complete complex formation. To elaborate on this series and as a control for this study, $[Fe(bpyPLA_2)_3]^{2+}$ was prepared with Cl^- and BF_4^-. Although $[Fe(bpyPLA_2)_3](BF_4)_2$ did not display a color change in CH_2Cl_2 and CH_2Cl_2/MeOH solvent systems, $[Fe(bpyPLA_2)_3]Cl_2$ did. Molar absorptivities for iron PLA and PEG-PLA block copolymer complexes in the respective solvents are compared in Table 4. Though there was no evidence of a precipitate in CH_2Cl_2 solutions, such small quantities of iron chloride salt could be difficult to detect visually. Thus, $[Fe(bpyPLA_2)_3]Cl_2$ and $[Fe(bpyPLA_2)_3](BF_4)_2$ were also analyzed by dynamic light scattering, but still there was no evidence of insoluble particles. Changes in the absorption spectra, specifically MLCT band broadening and decreased intensity, could indicate changes to the metal inner sphere in different solvents, perhaps chloro ligand involvement in nonpolar solvents, though typically that results in much more dramatic spectral changes.[48−52] Both mono(bpy)[48] and bis(bpy)[50−52] complexes give rise to spectra different from those observed here. In our experience, polymeric iron tris(bipyridine) complexes are not known to be solvatochromic. Previously color fading has been associated with polymeric iron tris(bipyridine) degradation; however, those processes are typically irreversible oxidations,[27] not reversible processes as noted here for MeOH addition.

Table 5. Thermal Analysis of bpy-Centered Macroligands and Iron Polymeric Complexes

polymer	M_n	T_m (°C)	T_d[a] (°C)	T_d'[b] (°C)
$bpyPEG_2$	5700	54	378	
bpy(PEG-PLA)$_2$	10000	38	222	372
	12300	33	231	371
	38500		256	384
[Fe{bpy(PEG-PLA)$_2$}$_3$]Cl$_2$	29800	36	164	359
	36900		183	366
	115600		230	378
$bpyPEG_2$	4800	54	366	
bpy(PEG-PLLA)$_2$	9100	38	220	375
	14600	34	218	375
	22900	151	261	370
[Fe{bpy(PEG-PLLA)$_2$}$_3$]Cl$_2$	27400	36	176	366
	43900	29	194	374
	68800	151	217	380

[a] Onset temperature for decomposition as determined by TGA. [b] Decomposition temperature of the second transition.

In addition to reversible solvent effects, previously we reported unexpected air sensitivity for $[Fe(bpyPEG_2)_3]SO_4$ in aqueous solution, with irreversible chromophore bleaching.[27] PEG complexes were stable under an argon atmosphere. To test whether similar effects are noted for block copolymers, iron sulfate complexes were prepared. Bpy(PEG-PLA)$_2$ macroligands with high PEG content were employed in this study, given their water solubility. [Fe{bpyPEG-PLA)$_2$}$_3$]SO_4 complexes were prepared by a previously reported procedure,[27] and their formation was monitored by UV−vis spectroscopy. Unlike $[Fe(bpyPEG_2)_3]SO_4$ complexes which formed and then degraded likely via radical processes in the presence of air, [Fe{bpyPEG-PLA)$_2$}$_3$]SO_4 complexes formed within minutes and were stable under ambient conditions.

Thermal Analysis. Thermal properties of PEG-PLA macroligands and iron complexes were analyzed by TGA and modulated DSC. The melting (T_m) and decomposition (T_d) temperatures are provided in Table 5. Thermal decomposition traces of block copolymer macroligands and iron complexes showed two transitions corresponding to decomposition of the PEG and PLA domains. The first transition at ∼200 °C is attributed to the decomposition of PLA or PLLA, while the second at ∼350 °C is for PEG. Upon metal complexation, a decrease in T_d was observed for both PLA and PLLA components. Although metals are known to increase the thermal stability of polymers,[53−55] this observation is consistent with other polymeric metal complexes reported in the literature.[56]

Melting temperatures for block copolymers with small PLA and PLLA segments are similar (∼35 °C). However, when the PLA block is large, no T_m is observed. For PLLA a T_m is seen at 151 °C due to the crystallinity of the stereoregular block domain. The thermal properties of PEG and PLA[57] blocks are in accord with literature values.[58]

Nanoparticles. Micelle-like nanoparticles of PLA-PEG-PLA are commonly prepared by nanoprecipitation in either acetone or DMF. Venkatraman et al.[8] showed that PLA-PEG-PLA micelle-like nanoparticles can be prepared using either DMF or DMAc, which are then removed by dialysis rather than in vacuo as is common for acetone or THF. Nanoparticles thus fabricated tend to be more uniform in size and smaller in diameter versus those of acetone or THF preparations. They concluded that the high polarity indices of DMF and DMAc solvents caused efficient solvent diffusion and polymer dispersion in water.[59] On the basis of these findings, both acetone and DMF were explored as solvents in PEG-PLA macroligand and iron complex nanoparticle preparations. Nanoparticles

Table 6. Hydrodynamic Diameters and Polydispersities of PEG-PLA Block Copolymer Nanoparticles[a]

polymer	M_n	particle size (nm)	polydispersity
bpy(PEG-PLA)$_2$	9900	—[b]	—[b]
	12300	113	0.15
	38500	156	0.07
bpy(PEG-PLLA)$_2$	9100	128	0.15
	14600	253	0.31
	22900	111	0.11
[Fe{bpy(PEG-PLA)$_2$}$_3$]Cl$_2$	29800	—[b]	—[b]
	36900	75	0.41
	115600	49	0.21
[Fe{bpy(PEG-PLLA)$_2$}$_3$]Cl$_2$	27400	51	0.45
	43900	37	0.42
	68800	61	0.20

[a] Data reported represent an average of three runs. [b] Particles were not observed in DLS measurements.

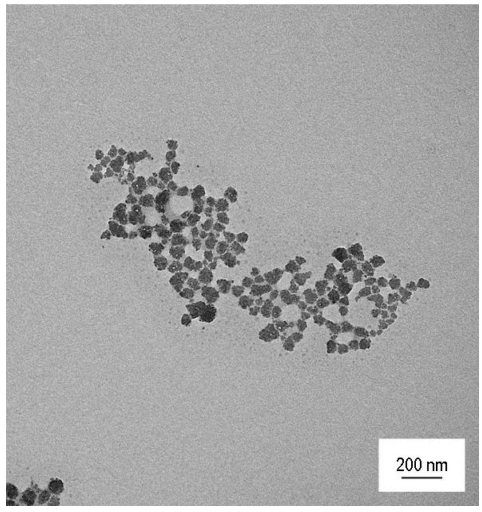

Figure 10. TEM image of bpy(PEG-PLA)$_2$ macroligand nanoparticles (M_n = 12 300).

prepared with acetone resulted in visible aggregates and large size distributions. Although DMF is suitable for preparing nanoparticles from macroligands, it is not compatible with iron complexes. [Fe{bpy(PEG-PLA)$_2$}$_3$]$^{2+}$ and [Fe{bpy(PEG-PLLA)$_2$}$_3$]$^{2+}$ are soluble in various nonpolar organic solvents including $CHCl_3$, CH_2Cl_2, toluene, DMSO, DMF, and THF, but when dissolved in DMF, the complexes are unstable, as is evidenced by bleaching of the red-violet iron tris(bipyridine) chromophores. During the precipitation procedure with DMF, the iron complexes degraded and DLS analysis showed a large particle size distribution. Additionally, solvents that can form peroxide (e.g., THF, dioxane) or acid (e.g., $CHCl_3$) impurities are also known to degrade the iron complexes.[27,32,60−62]

As an alternative, DMSO was explored in attempts to prevent chromophore degradation and produce particles with small hydrodynamic radii and narrower size distributions. For PLGA and PLA materials, DMSO has proven to be a useful solvent due to its high polarity index, producing uniform and small particles.[63] Using the nanoprecipitation method, block copolymer macroligands and iron complexes were dissolved in DMSO and added dropwise to stirred, distilled water. Samples were then dialyzed against water overnight to remove the DMSO. Macroligand suspensions of bpy(PEG-PLA)$_2$ and bpy(PEG-PLLA)$_2$ resulted in white turbid mixtures, and iron complexes [Fe{bpy(PEG-PLA)$_2$}$_3$]$^{2+}$ and [Fe{bpy(PEG-PLLA)$_2$}$_3$]$^{2+}$ formed transparent pink solutions. Additionally, DMSO did not degrade the labile iron(II) complexes, as evidenced by retention of the red-violet color. The micelle-like nanoparticles were analyzed by DLS to determine the hydrodynamic diameter and polydispersity (PD). DLS analysis verified that nanoparticles of bpy(PEG-PLA)$_2$ and bpy(PEG-PLLA)$_2$ were produced (111−253 nm diameter, PD ≤ 0.31) (Table 6). Nanoparticles of [Fe{bpy(PEG-PLA)$_2$}$_3$]$^{2+}$ and [Fe{bpy(PEG-PLLA)$_2$}$_3$]$^{2+}$ are smaller (37−75 nm diameter range) than those of bpy(PEG-PLA)$_2$ and bpy(PEG-PLLA)$_2$, and the polydispersities were ≤0.45. The range of nanoparticle sizes and spheroidal morphology were confirmed by TEM (Figures 10 and 11). When the PEG content is large in bpy(PEG-PLA)$_2$ (M_n = 9100) and [Fe{bpy(PEG-PLA)$_2$}$_3$]$^{2+}$ (M_n = 29 800), the materials are soluble in water and particles do not form. Bpy(PEG-PLA)$_2$ and bpy(PEG-PLLA)$_2$ nanoparticles are comparable in size but possess lower polydispersities than those made from linear PLA-PEG-PLA triblocks.[8] Compared to prior reports involving four-arm PEG-PLA stars of similar molecular weights, smaller diameters and comparable polydispersities were obtained for nanoparticles made from [Fe{bpy(PEG-PLA)$_2$}$_3$]$^{2+}$ and [Fe{bpy(PEG-PLLA)$_2$}$_3$]$^{2+}$ six-arm star blocks.[9]

To test materials stability to fabrication conditions, nanoparticle suspensions were freeze-dried and analyzed by GPC, ^{1}H NMR, and UV−vis spectroscopy. GPC analysis of macroligands and iron complexes revealed that the preparation did not degrade the polymer chains. Due to the chemical instability of iron tris(bipyridine) complexes to peroxides in THF and of labile polymeric metal complexes to the shear forces of high-pressure

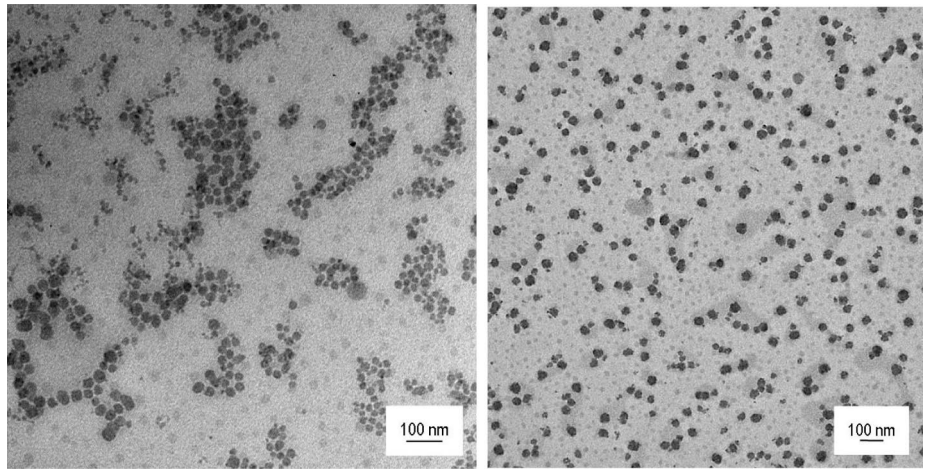

Figure 11. TEM images of [Fe{bpy(PEG-PLA)$_2$}$_3$]Cl$_2$ nanoparticles (M_n = 37 000). The presence of halolike regions surrounding the nanoparticles and a distribution of lighter particles between the nanoparticles suggest that a fraction of the polymer is dissolved in the nanoparticle dispersion and aggregates during solvent evaporation.

columns, macroligands typically dissociate from the iron centers during GPC analysis.[64] Thus, chromatograms of block copolymer Fe tris(bpy) complexes correspond to the bpy(PEG-PLA)$_2$ macroligand constituents. The molecular weights of PEG-PLA macroligands are comparable before and after nanoparticle preparation. ^{1}H NMR spectroscopy suggests that the dialysis and freeze-drying procedure were effective in removing the DMSO and water. Additionally, the molar absorptivity of Fe PEG-PLA nanoparticle samples analyzed in CH_2Cl_2/MeOH (3:1) after freeze-drying (10 300 M^{-1} cm^{-1}) is only slightly lower than that of the starting materials (11 600 M^{-1} cm^{-1}). Therefore, these studies show that nanoparticle preparation and freeze-drying processes have little effect on the metal center, polymer, and overall quality of the polymeric metal complex materials.

Summary

Well-defined bpyPLA$_2$, bpyPEG$_2$, and block copolymer bpy(PEG-PLA)$_2$ and bpy(PEG-PLLA)$_2$ macroligands were prepared via controlled ring opening polymerization methods, as confirmed by GPC and ^{1}H NMR analysis. Block copolymer macroligands were combined with iron(II) salts to produce metal site-isolated [Fe{bpyPEG-PLA)$_2$}$_3$]Cl$_2$ and [Fe{bpyPEG-PLLA)$_2$}$_3$]Cl$_2$ complexes. The formation of iron(II) tris(bipyridine)-centered complexes was evaluated by UV−vis spectroscopy. In a CH_2Cl_2/MeOH (3:1) cosolvent system, spectral properties of [Fe{bpyPEG-PLA)$_2$}$_3$]Cl$_2$ and [Fe{bpyPEG-PLLA)$_2$}$_3$]Cl$_2$ are comparable to those of the $[Fe(bpy)_3]^{2+}$ parent compound. However, lower molar absorptivities and broadened MLCT absorption bands were observed in CH_2Cl_2 solution. Homopolymer controls of [Fe(bpyPLA$_2$)$_3$]Cl$_2$ and [Fe(bpyPLA$_2$)$_3$](BF$_4$)$_2$ were prepared and analyzed by UV−vis spectroscopy in CH_2Cl_2 and 3:1 CH_2Cl_2/MeOH solutions. Complexes with chloride counterions exhibited changes in spectral properties in these solvent systems, whereas no change was observed for iron(II) complexes with BF_4^- counterions, illustrating that counterions can play a role in the spectral properties of iron PMCs in different solvents.

Micelle-like nanoparticles of bpy(PEG-PLA)$_2$, bpy(PEG-PLLA)$_2$, [Fe{bpyPEG-PLA)$_2$}$_3$]Cl$_2$, and [Fe{bpyPEG-PLLA)$_2$}$_3$]Cl$_2$ were prepared via a nanoprecipitation method using DMSO as the organic solvent. Suspensions were analyzed by DLS to determine particle sizes and distributions. Particles prepared from linear polymers of bpy(PEG-PLA)$_2$ and bpy(PEG-PLLA)$_2$ ranged from 111 to 253 nm in diameter with typical polydispersity indices of ∼0.15. Star block copolymers of [Fe{bpyPEG-PLA)$_2$}$_3$]Cl$_2$ and [Fe{bpyPEG-PLLA)$_2$}$_3$]Cl$_2$ afforded smaller nanoparticles (range 37−75 nm) compared to linear macroligand precursors. The range of nanoparticle sizes and spheroidal morphology were confirmed by TEM imaging. GPC, ^{1}H NMR, and UV−vis spectral analysis of freeze-dried nanoparticle suspensions suggested that nanoprecipitation methods do not compromise the integrity of the polymeric iron complex materials.

These polymers serve as models for a new kind of responsive drug delivery system. Amphiphilic materials form micelle-like nanoparticles that could entrap hydrophobic drugs. The introduction of a metal center introduces a chromophore and a responsive cross-link into the polymer architecture. Upon internalization into acidic intracellular lysosome environments, drug release could be facilitated by polymeric metal complex fragmentation accompanied by color bleaching and iron release, which could also influence biological processes and materials degradation by hydrolysis or radical mechanisms.

Acknowledgment. We thank the National Science Foundation (Grants BES 0402212, CHE 0350121, and CHE-0718879) for support of this research and GlaxoSmithKline for a summer undergraduate research award to J.L.K. We are grateful to Prof. Edwin L. Thomas and Daniel Alcazar (Massachusetts Institute of Technology) for TEM analysis of nanoparticle suspensions. Dr. Anne Pfister (University of Virgina) is acknowledged for her advice and contributions. We thank Prof. Marc A. Hillmyer and Dr. Huiming Mao (University of Minnesota) and Mr. William Shoup (University of Virginia) for advice and assistance with the ethylene oxide polymerization apparatus and procedure.

Supporting Information Available: Images of the ethylene oxide anionic polymerization apparatus and [Fe{bpyPEG-PLA)$_2$}$_3$]Cl$_2$, [Fe(bpyPLA$_2$)$_3$]Cl$_2$, [Fe(bpyPLA$_2$)$_3$](BF$_4$)$_2$ solvent and counterion effects. This material is available free of charge via the Internet at http://pubs.acs.org.

References and Notes

(1) Förster, S.; Plantenberg, T. *Angew. Chem., Int. Ed.* **2002**, *41*, 688–714.
(2) Ahmed, F.; Pakunlu, R. I.; Srinivas, G.; Brannan, A.; Bates, F.; Klein, M. L.; Minko, T.; Discher, D. E. *Mol. Pharmaceutics* **2006**, *3*, 340–350.
(3) Ahmed, F.; Discher, D. E. *J. Controlled Release* **2004**, *96*, 37–53.
(4) Geng, Y.; Discher, D. E. *J. Am. Chem. Soc.* **2005**, *127*, 12780–12781.
(5) Discher, D. E.; Ahmed, F. *Annu. Rev. Biomed. Eng.* **2006**, *8*, 323–341.
(6) Geng, Y.; Discher, D. E. *Polymer* **2006**, *47*, 2519–2525.
(7) Luo, L.; Tam, J.; Maysinger, D.; Eisenberg, A. *Bioconjugate Chem.* **2002**, *13*, 1259–1265.
(8) Venkatraman, S. S.; Jie, P.; Min, F.; Freddy, B. Y. C.; Leong-Huat, G. *Int. J. Pharm.* **2005**, *298*, 219–232.
(9) Jie, P.; Venkatraman, S. S.; Min, F.; Freddy, B. Y. C.; Huat, G. L. *J. Controlled Release* **2005**, *110*, 20–33.
(10) He, G.; Ma, L. L.; Pan, J.; Venkatraman, S. *Int. J. Pharm.* **2007**, *334*, 48–55.
(11) Ma, L. L.; Jie, P.; Venkatraman, S. S. *Adv. Funct. Mater.* **2008**, *18*, 716–725.
(12) Anseth, K. S.; Metters, A. T.; Bryant, S. J.; Martens, P. J.; Elisseeff, J. H.; Bowman, C. N. *J. Controlled Release* **2002**, *78*, 199–209.
(13) Peppas, N. A.; Huang, Y.; Torres-Lugo, M.; Ward, J. H.; Zhang, J. *Annu. Rev. Biomed. Eng.* **2000**, *2*, 9–29.
(14) Sanabria-DeLong, N.; Agrawal, S. K.; Bhatia, S. R.; Tew, G. N. *Macromolecules* **2006**, *39*, 1308–1310.
(15) Tew, G. N.; Sanabria-DeLong, N.; Agrawal, S. K.; Bhatia, S. R. *Soft Matter* **2005**, *1*, 253–258.
(16) Agrawal, S. K.; Sanabria-DeLong, N.; Tew, G. N.; Bhatia, S. R. *Macromolecules* **2008**, *41*, 1774–1784.
(17) Agrawal, S. K.; Sanabria-DeLong, N.; Jemian, P. R.; Tew, G. N.; Bhatia, S. R. *Langmuir* **2007**, *23*, 5039–5044.
(18) Kissel, T.; Li, Y.; Unger, F. *Adv. Drug Delivery Rev.* **2002**, *54*, 99–134.
(19) Kim, K.; Yu, M.; Zong, X.; Chiu, J.; Fang, D.; Seo, Y.-S.; Hsiao, B. S.; Chu, B.; Hadjiargyrou, M. *Biomaterials* **2003**, *24*, 4977–4985.
(20) Kim, K.; Luu, Y. K.; Chang, C.; Fang, D.; Hsiao, B. S.; Chu, B.; Hadjiargyrou, M. *J. Controlled Release* **2004**, *98*, 47–56.
(21) Wiggins, J. S.; Hassan, M. K.; Mauritz, K. A.; Storey, R. F. *Polymer* **2006**, *47*, 1960–1969.
(22) Valko, M.; Morris, H.; Cronin, M. T. D. *Curr. Med. Chem.* **2005**, *12*, 1161–1208.
(23) Wardman, P.; Candeias, L. P. *Radiat. Res.* **1996**, *145*, 523–531.
(24) Sen, C. K.; Khanna, S.; Babior, B. M.; Hunt, T. K.; Ellison, E. C.; Roy, S. *J. Biol. Chem.* **2002**, *277*, 33284–33290.
(25) Kemsley, J. N.; Zaleski, K. L.; Chow, M. S.; Decker, A.; Shishova, E. Y.; Wasinger, E. C.; Hedman, B.; Hodgson, K. O.; Solomon, E. I. *J. Am. Chem. Soc.* **2003**, *125*, 10810–10821.
(26) Cho, M.; Hunt, T. K.; Hussain, M. Z. *Am. J. Physiol. Heart Circ. Physiol.* **2001**, *280*, H2357–2363.
(27) Pfister, A.; Fraser, C. L. *Biomacromolecules* **2006**, *7*, 459–468.
(28) Fiore, G. L.; Klinkenberg, J. L.; Pfister, A.; Fraser, C. L. *Biomacromolecules*, submitted for publication.
(29) Smith, A. P.; Corbin, P. S.; Fraser, C. L. *Tetrahedron Lett.* **2000**, *41*, 2787–2789.
(30) Yasugi, K.; Nakamura, T.; Nagasaki, Y.; Kato, M.; Kataoka, K. *Macromolecules* **1999**, *32*, 8024–8032.
(31) Pangborn, A. B.; Giardello, M. A.; Grubbs, R. H.; Rosen, R. K.; Timmers, F. J. *Organometallics* **1996**, *15*, 1518–1520.
(32) Corbin, P. S.; Webb, M. P.; McAlvin, J. E.; Fraser, C. L. *Biomacromolecules* **2001**, *2*, 223–232.
(33) Hillmyer, M. A.; Bates, F. S. *Macromolecules* **1996**, *29*, 6994–7002.

(34) Reuter, H.; Höring, S.; Ulbricht, J. *Eur. Polym. J.* **1989**, *25*, 1113–1117.
(35) Nikos, H.; Marinos, P.; Hermis, I. *Adv. Polym. Sci.* **2005**, *189*, 1–124.
(36) Kataoka, K.; Harada, A.; Nagasaki, Y. *Adv. Drug Delivery Rev.* **2001**, *47*, 113–131.
(37) Hermanson, G. T. *Bioconjugate Techniques*; Academic Press: San Diego, 1996; p 785.
(38) Zalipsky, S. *Bioconjugate Chem.* **1995**, *6*, 150–165.
(39) Roberts, M. J.; Bentley, M. D.; Harris, J. M. *Adv. Drug Delivery Rev.* **2002**, *54*, 459–476.
(40) Harris, J. M.; Martin, N. E.; Modi, M. *Clin. Pharmacokinet.* **2001**, *40*, 539–551.
(41) Lin-Gibson, S.; Bencherif, S.; Cooper, J. A.; Wetzel, S. J.; Antonucci, J. M.; Vogel, B. M.; Horkay, F.; Washburn, N. R. *Biomacromolecules* **2004**, *5*, 1280–1287.
(42) Lin-Gibson, S.; Bencherif, S.; Antonucci, J. M.; Jones, R. L.; Horkay, F. *Macromol. Symp.* **2005**, *227*, 243–254.
(43) Lin-Gibson, S.; Jones, R. L.; Washburn, N. R.; Horkay, F. *Macromolecules* **2005**, *38*, 2897–2902.
(44) Bryant, S. J.; Chowdhury, T. T.; Lee, D. A.; Bader, D. L.; Anseth, K. S. *Ann. Biomed. Eng.* **2004**, *32*, 407–417.
(45) Johnson, R. M.; Fraser, C. L. *Macromolecules* **2004**, *37*, 2718–2727.
(46) Johnson, R. M.; Pfister, A.; Fraser, C. L. In *Metal-Containing and Metallosupramolecular Polymers and Materials*; Schubert, U. S., Newkome, G. R., Manner, I., Eds.; American Chemical Society: Washington, DC, 2006; Vol. *928*, pp 17−29.
(47) Meier, M. A. R.; Wouters, D.; Ott, C.; Guillet, P.; Fustin, C. A.; Gohy, J. F.; Schubert, U. S. *Macromolecules* **2006**, *39*, 1569–1576.
(48) Krumholz, P. *J. Am. Chem. Soc.* **1949**, *71*, 3654–3656.
(49) Baxendale, J. H.; Bridge, N. K. *J. Phys. Chem.* **1955**, *59*, 783–788.
(50) Baxendale, J. H.; George, P. *Trans. Faraday Soc.* **1950**, *46*, 55–63.
(51) Konig, E. *Coord. Chem. Rev.* **1968**, *3*, 471–495.
(52) Nguyen, T. H.; Shannon, P. J.; Hoggard, P. E. *Inorg. Chim. Acta* **1999**, *291*, 136–141.
(53) Cyr, P. W.; Tzolov, M.; Hines, M. A.; Manners, I.; Sargent, E. H.; Scholes, G. D. *J. Mater. Chem.* **2003**, *13*, 2213–2219.
(54) Hofmeier, H.; Wouters M. ; Wouters, D.; Schubert U. S. In *Metal-Containing and Metallosupramolecular Polymers and Materials*; Schubert, U. S., Newkome, G. R., Manners, I., Eds.; American Chemical Society: Washington, DC, 2006; Vol. *928*, pp 113−125.
(55) Qin, Y.; Cui, C.; Jäkle, F. *Macromolecules* **2008**, *41*, 2972–2974.
(56) Fiore, G. L.; Fraser, C. L. *Macromolecules* **2008**, *41*, 7892−7897.
(57) Jamshidi, K.; Hyon, S. H.; Ikada, Y. *Polymer* **1988**, *29*, 2229–2234.
(58) Sanabria-DeLong, N.; Aamer, K. A.; Agrawal, S. K.; Bhatia, S. R.; Tew, G. N. In *Degradable Polymers and Materials*; Khemani, K., Scholz, C., Eds.; American Chemical Society: Washington, DC, 2006; Vol. *939*.
(59) Cheng, J.; Teply, B. A.; Sherifi, I.; Sung, J.; Luther, G.; Gu, F. X.; Levy-Nissenbaum, E.; Radovic-Moreno, A. F.; Langer, R.; Farokhzad, O. C. *Biomaterials* **2007**, *28*, 869–876.
(60) McAlvin, J. E.; Scott, S. B.; Fraser, C. L. *Macromolecules* **2000**, *33*, 6953–6964.
(61) McAlvin, J. E.; Fraser, C. L. *Macromolecules* **1999**, *32*, 1341–1347.
(62) Fraser, C. L.; Smith, A. P. *J. Polym. Sci., Part A: Polym. Chem.* **2000**, *38*, 4704–4716.
(63) Ataman-Onal, Y.; Munier, S.; Ganee, A.; Terrat, C.; Durand, P.-Y.; Battail, N.; Martinon, F.; Le Grand, R.; Charles, M.-H.; Delair, T.; Verrier, B. *J. Controlled Release* **2006**, *112*, 175–185.
(64) Lamba, J. J. S.; Fraser, C. L. *J. Am. Chem. Soc.* **1997**, *119*, 1801–1802.

MA801721Q